J|A|C|S
ARTICLES
Published on Web 08/27/2004

Mechanistic Analysis of Hydroarylation Catalysts

Jonas Oxgaard,[†] Roy A. Periana,[‡] and William A. Goddard, III*,[†]

Contribution from the Materials and Process Simulation Center, Beckman Institute (139-74), Division of Chemistry and Chemical Engineering, California Institute of Technology, Pasadena, California 91125, and Department of Chemistry, Loker Hydrocarbon Institute, University of Southern California, Los Angeles, California 90089

Received March 1, 2004; E-mail: wag@wag.caltech.edu

Abstract: Recently, two organometallic systems ([Ir(μ-acac-O)(acac-O,O)(acac-C^3)]$_2$ and (Tp)Ru(CO)(Ph)-(NCCH$_3$)) have been discovered that catalyze hydroarylation of unactivated olefins. Herein, we use density functional theory (B3LYP) to study the factors underlying this class of catalysts. In addition, we calculate the key steps for Rh, Pd, Os, and Pt with similar ligand sets. We previously showed there to be two key steps in the process: (i) insertion of a phenyl into the π bond of a coordinating olefin, and (ii) C−H activation/hydrogen transfer of an unactivated benzene. An important discovery in these studies is that the barriers for these two steps are inversely correlated, complicating optimization of the overall process. However, herein we elucidate the causes of this inverse correlation, laying the foundation for the rational design of improved catalysts. Both steps are directly influenced by the accessibility of the higher 2-electron oxidation state, $M^n \rightarrow M^{n+2}$. Systems with an easily accessible M^{n+2} state activate C−H bonds easily but suffer from high energy insertions due to significant back-bonding. Conversely, systems without an easily accessible M^{n+2} state have no debilitating back-bonding which makes insertion steps facile, but cannot effectively activate the C−H bond (leading instead to polymerization). The relationship between accessibility of the M^{n+2} state and the amount of back-bonding in the coordinating olefin can be visualized by inspecting the hybridization of the coordinating olefin. Furthermore, we find a linear relation between this hybridization and the barrier to insertion. On the basis of these concepts, we suggest some modifications of the σ framework expected to improve the rates beyond this linear correlation.

1. Introduction

Over the past decade, significant effort has been directed toward functionalization of unactivated C−H bonds by transition metal complexes.[1] More recently, a novel subset of C−H functionalization processes has been reported − hydroarylation of olefins (Figure 1), a process that couples an olefin to an unactivated aryl. However, none of the catalysts currently available are sufficiently active and/or selective to be commercially viable. In this report, we explore the general themes for this class of catalysts and what this mechanism suggests for strategies to design a better system.

The first reported hydroarylation catalyst is the binuclear complex [Ir(μ-acac-O)(acac-O,O)(acac-C^3)]$_2$ (Ir•acac) reported by Matsumoto et al.[2] Heating a benzene solution of Ir•acac and 1.7 MPa of ethene to 180 °C for 3 h led to ethyl benzene with

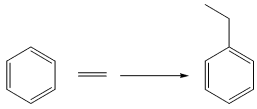

Figure 1. Hydroarylation of olefin.

a reported turnover frequency (TOF) of 421 × 10^{-4} s^{-1}, and an activation energy of 28.7 kcal/mol.[3,4]

Later variations of this system by Periana et al.[5] featured several mononuclear Ir compounds of the form Ir(acac-O,O)$_2$-(R)(L), where R is either (acac-O,O,C^3) or Ph, and L is either H_2O or pyridine (see Figure 2). The systems where L = H_2O showed higher activity than the dinuclear and pyridine containing variants. This group has in a later study concluded that the Ir•acac-based catalysts share a common mechanism, and attributed the higher activity of the H_2O ligand to a ground-state effect.[6] Because these Ir-based systems share a common mechanism, they will be collectively referred to as Ir•acac.

More recently, Gunnoe and co-workers reported a new catalyst for the same reaction, (Tp)Ru(CO)(Ph)(NCCH$_3$) (Ru•Tp•CO) (Tp = hydridotris (pyrazolyl) borate), which, with an

[†] California Institute of Technology.
[‡] University of Southern California.

(1) (a) Crabtree, R. H. *J. Chem. Soc., Dalton Trans*. **2001**, 2437. (b) Crabtree, R. H. *Chem. Rev*. **1995**, *95*, 987. (c) Meyer, T. Y.; Woerpel, K. A.; Novak, B. M.; Bergman, R. G. *J. Am. Chem. Soc*. **1994**, *116*, 10290. (d) Jones, W. D.; Hessell, E. T. J. *J. Am. Chem. Soc.* **1992**, *114*, 6087. (e) Kozhevnikov, I. V.; Kim, V. I.; Talzi, E. P.; Sidelnikov, V. N. *J. Chem. Soc., Chem. Commun.* **1985**, 1392. (f) Gretz, E.; Oliver, T. F.; Sen, A. *J. Am. Chem. Soc.* **1987**, *109*, 8109. (g) Crabtree, R. H. *Chem. Rev*. **1985**, *85*, 245.
(2) Matsumoto, T.; Taube, D. J.; Periana, R. A.; Taube, H.; Yoshida, H. *J. Am. Chem. Soc*. **2000**, *122*, 7414.
(3) Matsumoto, T.; Periana, R. A.; Taube, D. J.; Yoshida, H. *J. Mol. Catal. A* **2002**, 1.
(4) Matsumoto, T.; Yoshida, H. *Catal. Lett*. **2001**, *72*, 107.
(5) Periana, R. A.; Liu, Y. X.; Bhalla, G. *Chem. Commun*. **2002**, 3000.
(6) Oxgaard, J.; Muller, R. P.; Periana, R. A.; Goddard, W. A., III. *J. Am. Chem. Soc*. **2004**, *126*, 352.

10.1021/ja048841j CCC: $27.50

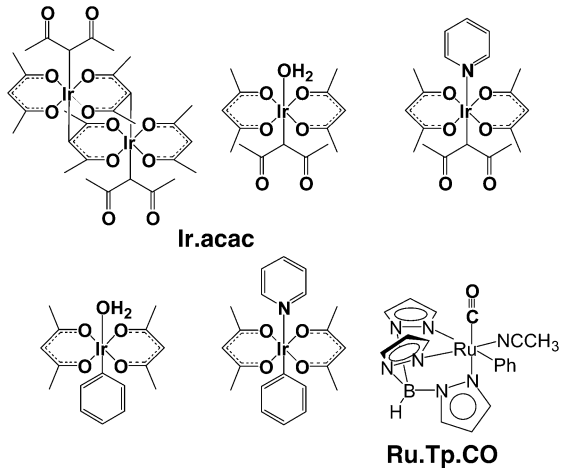

Figure 2. Derivatives of Ir·acac and Ru·Tp·CO.

ethene pressure of only 0.17 MPa, at 90 °C yields ethyl benzene with a TOF of 3.5×10^{-3} s^{-1}.[7] Comparing this TOF to a TOF for Ir·acac (extrapolated to 90 °C from ref 3) suggests that Ru·Tp·CO is ~200 times faster than Ir·acac. However, Ru·Tp·CO is not stable, over time forming an as-of-yet unidentified high-spin species. Furthermore, theoretical studies by this group indicated that significant oligomerization should occur at higher ethylene pressures,[8] which was later confirmed experimentally.[9]

Our theoretical studies of Ir·acac[6] and Ru·Tp·CO[8] have shown that they react through a common mechanism, illustrated in Figure 3. This mechanism, starting from a complex with a covalently bound phenyl and an η-2 coordinating olefin (A), features a 1,2-insertion of the phenyl into the ethene (TS1) to a chelating complex (B), rotation of the C−C bond to open up a vacant site (C), η-2 coordination of a benzene (D), migration of an aryl hydrogen (TS2), and regeneration of the active catalyst (E → F → A).

TS1 is the rate-determining step in both cases, with calculated activation energies of 27.0 and 24.9 kcal/mol, respectively, in addition to ground-state effects. TS1 is a classical insertion transition structure of the type observed for polymerizations, Heck insertions, etc., formally classified as $2_s + 2_s$ rearrangements.[10] Our previous studies[6,8] have also shown that TS1 is responsible for the observed regioselectivity when substituted olefins are used. Both Ir·acac and Ru·Tp·CO feature a transition state with a region of empty space where a bulky substituent prefers to be located, leading to primarily linear product.

TS2, the C−H activation step for the two systems, has activation energies of 14.1 (Ir·acac) and 15.9 (Ru·Tp·CO) kcal/mol, with respect to A. However, with respect to the previous intermediate, D, the activation energies are 12.0 and 18.8 kcal/mol, respectively. These barriers will henceforth be referred to as ΔH(TS1−A) and ΔH(TS2−D).

The mechanism for TS2 is in both cases oxidative hydrogen migration (OHM) − a concerted transfer of a hydrogen from the aryl carbon to the aliphatic carbon, with a transition structure reminiscent of but not identical to an oxidative addition (OA). The presence of a fully formed M−H bond is incompatible with a σ-bond metathesis mechanism, while the presence of partial C−H bonds and the absence of a stable M^{n+2} intermediate is incompatible with OA. In $TS2_{Ir\cdot acac}$ M−H = 1.58 Å, RCH_2−H = 1.69 Å, and C_{Ph}−H = 1.99 Å, while in $TS2_{Ru\cdot Tp\cdot CO}$ M−H = 1.61 Å, RCH_2−H = 1.65 Å, and C_{Ph}−H = 1.56 Å.

As was outlined previously,[6] the OHM mechanism is related to OA and occurs when the OA intermediate is disfavored by electronic or steric factors, as illustrated in Figure 4. This is reflected in shorter C−H bond lengths in $TS2_{Ru\cdot Tp\cdot CO}$ as compared to $TS2_{Ir\cdot acac}$: $TS2_{Ru\cdot Tp\cdot CO}$ has higher energy and is consequently further away from a true intermediate than is $TS2_{Ir\cdot acac}$.[11] A more detailed study of the OHM mechanism and its relation to OA is currently under preparation for submission.

Our previous work on these systems elucidated the mechanism for the two catalyst classes separately, but we now consider the larger issue: What are the fundamental themes of a functional hydroarylation catalyst? Considering the wealth of systems capable of catalyzing insertions of activated aryls (such as Heck reaction catalysts) and systems capable of catalyzing C−H activation (such as the Bergman iridium Cp system), why are these two catalyst classes the only two that can catalyze both?

In particular, this paper will address the following questions:

(i) Why is Ru·Tp·CO more active than Ir·acac?

(ii) Is the increase of $\Delta H(TS2-D)_{Ru\cdot Tp\cdot CO}$ related to the decrease of $\Delta H(TS1-A)_{Ru\cdot Tp\cdot CO}$ or merely a coincidence?

(iii) If there is such a relation, is it applicable to a larger class of catalysts or is it isolated to the Ru·Tp·CO/Ir·acac pair?

(iv) Is the presence of oligomerization in the Ru·Tp·CO system related to the more efficient insertion?

(v) Can a system be designed where both ΔH(TS1−A) and ΔH(TS2−D) are simultaneously lowered, and what would the characteristics of a system like this be?

2. Computational Methodology

All calculations were performed using the hybrid DFT functional B3LYP as implemented by the Jaguar 5.0 program package.[12] This DFT functional utilizes the Becke three-parameter functional[13] (B3) combined with the correlation functional of Lee, Yang, and Par[14] (LYP) and is known to produce good descriptions of reaction profiles for transition metal-containing compounds.[15,16] The metals were described by the Wadt and Hay[17] core-valence (relativistic) effective core potential (treating the valence electrons explicitly) using the LACVP basis set with the valence double-ζ contraction of the basis functions, LACVP**. All electrons were used for all other elements using a modified variant of Pople's[18] 6-31G** basis set, where the six d functions have been reduced to five.

Implicit solvent effects of the experimental benzene medium were calculated with the Poisson−Boltzmann (PBF) continuum approxima-

(7) Lail, M.; Arrowood, B. N.; Gunnoe, T. B. *J. Am. Chem. Soc.* **2003**, *125*, 7506.
(8) Oxgaard, J.; Goddard, W. A., III. *J. Am. Chem. Soc.* **2004**, *126*, 442.
(9) Lail, M.; Bell, C. M.; Conner, D.; Cundari, T. R.; Gunnoe, T. B.; Petersen, J. L., manuscript submitted for publication.
(10) Steigerwald, M. L.; Goddard, W. A., III. *J. Am. Chem. Soc.* **1985**, *107*, 5027.
(11) It should be noted that this does not necessarily imply the continuity between the oxidative addition and σ-bond metathesis mechanisms suggested by Lam et al. (*Chem.-Eur. J.* **2003**, *9*, 2775).
(12) Jaguar 5.0, Schrodinger, Inc., Portland, OR, 2000.
(13) Becke, A. D. *J. Chem. Phys.* **199**3, *98*, 5648.
(14) Lee, C.; Yang, W.; Parr, R. G. *Phys. Rev. B* **1988**, *37*, 785.
(15) Baker, J.; Muir, M.; Andzelm, J.; Scheiner, A. In *Chemical Applications of Density-Functional Theory*; Laird, B. B., Ross, R. B., Ziegler, T., Eds.; ACS Symposium Series 629; American Chemical Society: Washington, DC, 1996.
(16) Niu, S.; Hall, B. M. *Chem. Rev.* **2000**, *100*, 353.
(17) (a) Hay, P. J.; Wadt, W. R. *J. Chem. Phys.* **1985**, *82*, 299. (b) Goddard, W. A., III. *Phys. Rev.* **1968**, *174*, 659. (c) Melius, C. F.; Olafson, B. O.; Goddard, W. A., III. *Chem. Phys. Lett.* **1974**, *28*, 457.
(18) (a) Hariharan, P. C.; Pople, J. A. *Chem. Phys. Lett.* **1972**, *16*, 217. (b) Francl, M. M.; Pietro, W. J.; Hehre, W. J.; Binkley, J. S.; Gordon, M. S.; DeFrees, D. J.; Pople, J. A. *J. Chem. Phys.* **1982**, *77*, 3654.

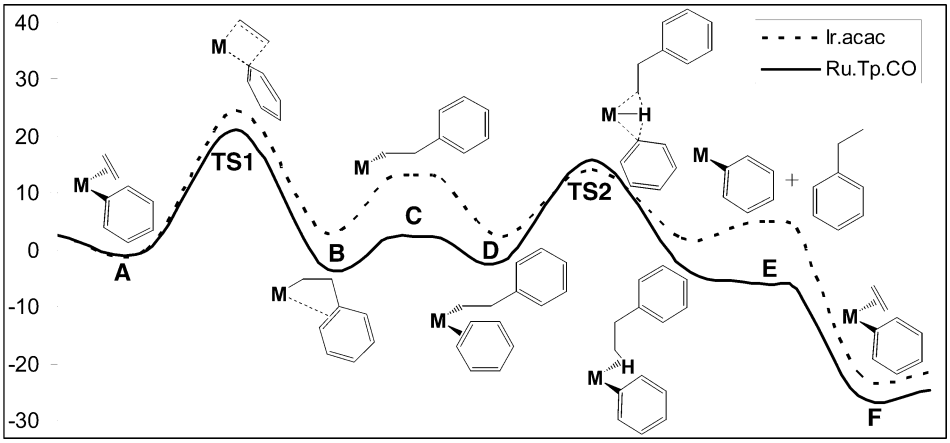

Figure 3. Reaction mechanism for Ir·acac and Ru·Tp·CO.

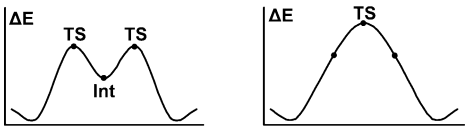

Figure 4. Comparison of the OA mechanism (left) to the OHM mechanism (right).

tion,[19] using the parameters $\epsilon = 2.284$ and $r_{solv} = 2.602$ Å. Due to the increased cost of optimizing systems in the solvated phase (increase in computation time by a factor of ~4), solvation effects are calculated here as single point solvation corrections to gas-phase geometries. Our previous work on the Ir·acac system has shown that the total energies, geometries, frequencies, and zero-point energies were also largely unchanged when the systems were optimized in the solvation phase.

All energies here are reported as ΔE + zero-point energy corrections at 0 K + solvation correction. Relative energies on the ΔH(0 K) surface are expected to be accurate to within 3 kcal/mol for stable intermediates, and within 5 kcal/mol for transition structures. Moreover, relative energies of iso-electronic species (such as regioisomers) are considerably more accurate, because the errors largely cancel.

Free energies are not included, due to the inadequacies of free energy calculations in solutions. A more thorough analysis of this can be found in ref 6. However, a free energy term is implicitly included in the PBF solvation methodology.

All geometries were optimized and evaluated for the correct number of imaginary frequencies through vibrational frequency calculations using the analytic Hessian. Zero imaginary frequencies correspond to a local minimum, while one imaginary frequency corresponds to a transition structure. Although the singlet states are expected to be the lowest energy spin states, we also investigated higher spin states for select geometries, and we invariably found the singlet as the lowest energy state.

To reduce computational time, the methyl groups on the acac ligands were replaced with hydrogens. Control calculations show that the relative energies of intermediates and transition structures change less than 0.1 kcal/mol when methyl groups are included.

3. Results and Discussion

Our previous work on the Ru·Tp·CO system[8] showed that it is more active than the Ir·acac system despite being more electron rich (with a calculated metal Mulliken charge of +0.07e vs +0.45e for the Ir·acac system). This is in stark contrast to the general view of late metal insertion catalysis, that is, that lower electron density leads to higher activity.[20] A well-known example is the Brookhart ethylene polymerization catalyst, which is active for polymerization only in its cationic state.[20]

One might consider explaining this behavior in terms of steric interactions in the Ir·acac transition state, which would raise the relative energy of $TS1_{Ir\cdot acac.}$ However, both systems are essentially unhindered, rendering sterics insignificant.

To understand this seemingly contradictory behavior, we investigated whether it is the metal or the ligand set that is most influential in improving the activity of Ru·Tp·CO. Calculations were carried out in which the metal center of the Ir·acac and Ru·Tp·CO systems was replaced with Ru and Ir, respectively. The systems were kept isoelectronic, with the Ir·Tp·CO system cationic ($Ir\cdot Tp\cdot CO^+$) and the Ru·acac system anionic ($Ru\cdot acac^-$). For comparison purposes, we considered only the actual insertion step, that is, A → B through TS1, ignoring all ground-state effects. The results, as illustrated in Table 1, show clearly that it is the ligand system that is responsible for the higher activity. Replacing the ruthenium in Ru·Tp·CO with $iridium^+$ lowered the activation energy from 21.1 to 17.0 kcal/mol, while replacing the iridium in Ir·acac with $ruthenium^-$ raised the activation energy from 24.5 to 28.3 kcal/mol.

We also observe that TS1 becomes a later transition state as the activation energy increases, in accordance to the Hammond postulate. The C1−C2 distance (the breaking π bond) is 1.44 Å for $Ir\cdot Tp\cdot CO^+$, and 1.49 Å for $Ru\cdot acac^-$. Furthermore, the C2−C3 distance (the forming C−C bond) decreases from 2.07 Å for $Ir\cdot Tp\cdot CO^+$ to 1.78 Å for $Ru\cdot acac^-$. Even more dramatic than the change in the activation energy is the change in the ΔH of the reaction, following the Bell−Evans−Polanyi principle. Converting A to B for $Ir\cdot Tp\cdot CO^+$ is exothermic by 9.5 kcal/mol, while for $Ru\cdot acac^-$ it is endothermic by 9.1 kcal/mol.

As mentioned above, Ru·Tp·CO leads to a lower ΔH(TS1−A) but a significantly higher ΔH(TS2−D). To test whether this is a pertinent observation or merely coincidental, we investigated ΔH(TS2−D) for $Ir\cdot Tp\cdot CO^+$ and $Ru\cdot acac^-$ as well. The results, summarized in Table 2, show clearly the presence of an inverse trend. As the ΔH(TS1−A) increases from $Ir\cdot Tp\cdot CO^+$ to $Ru\cdot acac^-$, ΔH(TS2−D) decreases. However, there is no correlation between ΔH(TS2−D) and the ΔH of the reaction D → E. This is reasonable, because the reaction is essentially thermoneutral, in contrast to the results for A → B.

(19) (a) Tannor, D. J.; Marten, B.; Murphy, R.; Friesner, R. A.; Sitkoff, D.; Nicholls, A.; Ringnalda, M.; Goddard, W. A., III; Honig, B. *J. Am. Chem. Soc.* **1994**, *116*, 11875. (b) Marten, B.; Kim, K.; Cortis, C.; Friesner, R. A.; Murphy, R. B.; Ringnalda, M. N.; Sitkoff, D.; Honig, B. *J. Phys. Chem.* **1996**, *100*, 11775.

(20) Ittel, S. D.; Johnson, L. K.; Brookhart, M. *Chem. Rev.* **2000**, *100*, 1169.

Table 1. Relative Energies and Pertinent Geometry Parameters for A → TS1 and A → B

	Δ*H*(TS1–A) (kcal/mol)	M–C1 (Å)	C1–C2 (Å)	C2–C3 (Å)	C3–M (Å)	Δ*H*(A → B) (kcal/mol)
Ir·Tp·CO$^+$	17.0	2.14	1.44	2.07	2.21	−9.5
Ru·Tp·CO	21.1	2.12	1.46	1.93	2.26	−2.9
Ir·acac	24.5	2.07	1.47	1.9	2.2	3.1
Ru·acac$^-$	28.3	2.06	1.49	1.78	2.26	9.1

Table 2. Relative Energies and Pertinent Geometry Parameters for D → TS2 and D → E

	Δ*H*(TS2–D) (kcal/mol)	M–H (Å)	H–CH_2R (Å)	M–CH_2R (Å)	H–Ph (Å)	M–Ph (Å)	Δ*H*(E → D) (kcal/mol)
Ir·Tp·CO$^+$	25.3	1.64	1.64	2.29	1.57	2.17	2.5
Ru·Tp·CO	18.0	1.61	1.65	2.27	1.56	2.17	−3.7
Ir·acac	11.8	1.56	1.70	2.20	1.95	2.09	−0.4
Ru·acac$^-$	6.9	1.55	1.68	2.19	1.87	2.09	−2.1

Table 3. Structural Data (Olefin Bond Length and Inversion Angle (Θ)) for the Substrate (A in Figure 3) and Activation Energies for Insertion (TS1−A), C−H Activation (TS2−D), and Polymerization (TS3−G) (A Positive Δ*H*(TS2−TS3) Indicates that C−H Activation Is Preferred over Polymerization)

ligand	metal	C1–C2 in A Å	Θ in A deg	Δ*H*(TS1–A) kcal/mol	Δ*H*(TS2–D) kcal/mol	Δ*H*(TS3–G) kcal/mol	Δ*H*(TS2–TS3) kcal/mol
M(acac)$_2$	Os(−)	1.42	15.00	40.1	0.7	48.3	20.5
	Ru(−)	1.40	11.20	28.3	6.9	30.0	4.0
	Ir	1.40	10.20	24.5	11.8	33.6	0.6
	Rh	1.37	7.00	14.6	19.6	21.8	−10.6
	Pt(+)	1.38	6.20	7.4	27.1	23.4	−11.9
	Pd(+)	1.37	4.35	3.4	26.5	14.5	−16.4
M·Tp·CO	Os	1.41	13.90	32.0	4.9	40.3	9.5
	Ru	1.39	10.15	21.1	18.0	27.6	−6.7
	Ir(+)	1.40	9.10	17.0	20.6	27.8	−8.5
	Rh(+)	1.37	6.50	10.8	24.2	20.4	−13.8

Having established that an inverse trend is present, we investigated the generality of this trend for elements other than iridium and ruthenium. As iridium seems to be more suited for this reaction than ruthenium (lower insertion energy with the same ligand set), we elected to study the elements Rh, Pd, Os, and Pt with the bis-acac ligand set. We also studied the elements Rh and Os with the Tp·CO ligand set. We kept all of the complexes isoelectronic, so, for example, Os·acac is an anion while Pt·acac is a cation. Note that this leads to an oxidation state of IV for Pd·acac$^+$ and Pt·acac$^+$.

The results of this study are summarized in Table 3. However, to illustrate the results, we plotted Δ*H*(TS1−A) versus Δ*H*(TS2−D), as shown in Figure 5. For all systems except the Os^{II} compounds, C−H activation occurs through an OHM mechanism. For the two Os^{II} compounds, we instead find very low-energy Os^{IV} intermediates, that is, the products of oxidation addition. In Figure 5 we included the energy of the intermediates and not the transition states leading to and from reactant/product, as we believe that the energy of the intermediates most accurately reflects the chemistry of these systems.

Figure 5 shows an excellent correlation (R^2 of 0.9240) between Δ*H*(TS1−A) and Δ*H*(TS2−D), with a linear fit of Δ*H*(TS1−A) = −1.05*Δ*H*(TS2−D) + 38. Furthermore, exclusion of the lowest point on the Δ*H*(TS1−A) axis (Pd·acac$^+$) improves the fit of the line (to R^2 = 0.9416), indicating that the correlation breaks down as Δ*H*(TS1−A) approaches zero. This is expected, because extrapolation of the line to values of Δ*H*(TS2−D) higher than 35 kcal/mol would lead to negative values of Δ*H*(TS1−A).

This correlation implies that Δ*H*(TS1−A) and Δ*H*(TS2−D) are influenced by a common factor. Because the slope of the line is −1.08 rather than −1, this factor is more important for Δ*H*(TS2−D) than for Δ*H*(TS1−A). Examining the extreme points of the line, we observe that systems with a high Δ*H*(TS1−A) and a low Δ*H*(TS2−D) (Os^{II}, Ru^{II}) have fairly easily accessible M^{n+2} states (Os^{IV}, Ru^{IV}), while systems with a low Δ*H*(TS1−A) and a high Δ*H*(TS2−D) (Pd^{IV}, Pt^{IV}) have fairly high-energy M^{n+2} states (Pd^{VI}, Pt^{VI}).

Because D → TS2 is an oxidative process, we expect that a more easily accessible M^{n+2} state will favor either an oxidative addition intermediate or an OHM transition state. Indeed, for

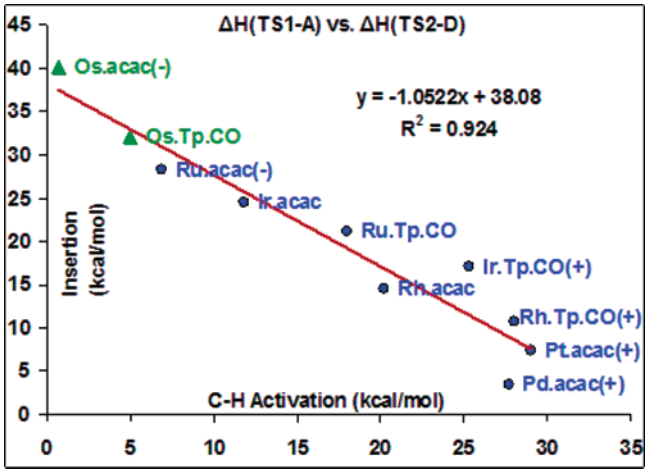

Figure 5. The correlation of the activation energy for insertion (Δ*H*(TS1−A)) versus the activation energy for C−H activation (Δ*H*(TS2−D)). The linear trend line fits the points with a correlation of R^2 = 0.9240. Catalysts in which the C−H activation is via OHM are in blue circles, whereas catalysts in which C−H activation is via oxidative addition (Os only) are shown in green triangles.

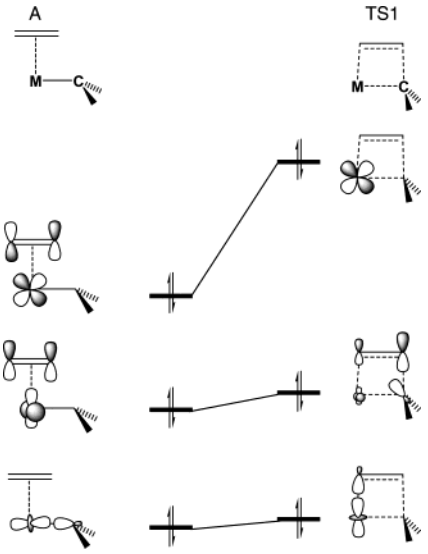

Figure 6. Simplified orbital analysis of A → TS1.

Os·acac⁻ oxidative addition is almost thermoneutral, and it will likely be exothermic for more electron-donating ligands. However, this is largely irrelevant, because the systems with sufficiently accessible M^{n+2} states would all have prohibitively high energy insertion steps.

This leaves the question of why a more easily accessible M^{n+2} state would increase the barrier for the insertion step, ΔH(TS1−A). The prerequisite for an easily accessible M^{n+2} state is a low-lying unoccupied d orbital. Moreover, a system with a low-lying unoccupied d orbital and a coordinating olefin would display a significant amount of back-bonding, which could increase the ΔH(TS1−A) through a ground-state effect. Orbital analysis of the transition from A → TS1 shows that all such back-bonding is lost in TS1, because there are no available unoccupied orbitals (see Figure 6). In this configuration, the olefin has slipped toward one side, forming an imperfect square and making the π^* orbital of the olefin unavailable. Consequently, a system with an easily accessible M^{n+2} state would exhibit significant back-bonding and a high-energy TS1.

To prove this hypothesis, we investigated the back-bonding to the olefin in A. We initially considered a traditional measurement of back-bonding, the C−C distance. The plot in Figure 7, ΔH(TS1−A) versus olefin bond length in A, shows that a trend is present ($R^2 = 0.8285$) but does not conclusively prove the presence of a correlation. This is most likely due to the varying amounts of forward bonding, which would influence the C−C distance but not ΔH(TS1−D).[21]

Instead, we correlated the amount of back-bonding to the amount of hybridization in the A complexes. Increasing amounts of back-bonding will increase the hybridization of the olefin carbons.[22] In the limit of very strong bonding, these back-bonded olefins can be thought of as a metallacyclopropanes, with sp^3 hybridized carbons. Indeed, the transformation of an η-2 coordinating olefin to a metallacyclopropane could be considered an oxidative process, which is consistent with the connection between a more accessible M^{n+2} state and a lower barrier to C−H activation. However, the amount of forward bonding is irrelevant, as even a strongly forward bonding complex remains planar.

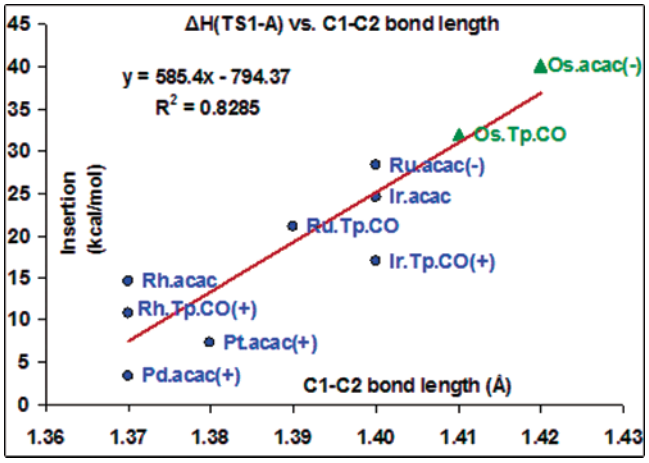

Figure 7. Activation energy of insertion (TS1−A) versus olefin bond length in A.

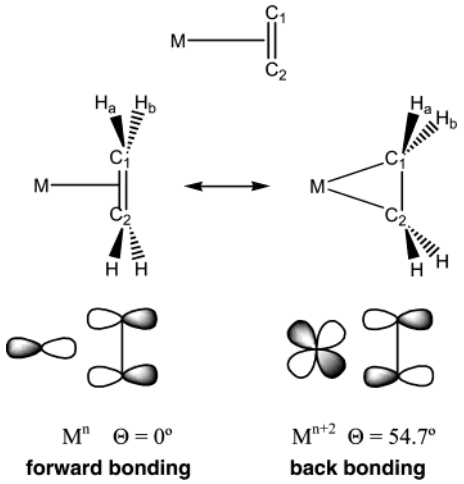

Figure 8. Inversion angle (Θ) in a back-bonding olefin.

The hybridization is measured as the inversion angle (Θ), as illustrated in Figure 8. In a purely forward bonding complex, the olefin carbons are sp^2 hybridized and thus completely planar, with Θ = 0°. The olefin carbons in a complex with significant back-bonding are sp^3 hybridized and thus pyramidal, with an "ideal" Θ = 54.7°.

Thus, to establish the connection between the amount of back-bonding and the barrier for insertion, Figure 9 plots Θ versus the ΔH(TS1−A). This shows a clear correlation ($R^2 = 0.9696$) in which systems with high-energy insertion barriers have relatively nonplanar olefins and consequently significant back-bonding. While we expect this correlation to break down at low values of Θ (because the linear correlation would lead to ΔH(TS1−A) ≤ 0 for values of Θ ≤ 3.3°), it works remarkably well even for Pd·acac⁺ and Pt·acac⁺.

Intriguingly, the accuracy of the linear fit (ΔH(TS1−A) = 3.31*Θ − 11.0) in Figure YY8 (average error 1.7 kcal/mol, max error 2.3 kcal/mol) suggests that Θ could be used to

(21) During review of this manuscript, a new report was published where the lack of correlation between back-bonding and olefin bond length was documented for olefin complexes to Cu, Ag, and Au. These authors found a better correlation by using NBO calculations of the bonding between metal and olefin (Kim, K. C.; Lee, K. A.; Kim, C. K.; Lee, B.; Lee, H. W. *Chem. Phys. Lett.* **2004**, *391*, 321).

(22) For example: (a) Collman, J. P.; Hegedus, L. S.; Norton, J. R.; Finke, R. G. *Principles and Applications of Organotransition Chemistry*; University Science Books: Mill Valley, CA, 1987; p 150. (b) Crabtree, R. H. *The Organometallic Chemistry of the Transition Metals*; Wiley: New York, 2001; p 107. (c) Yamamoto, A. *Organotransition Metal Chemistry*; Wiley: New York, 1986; p 220

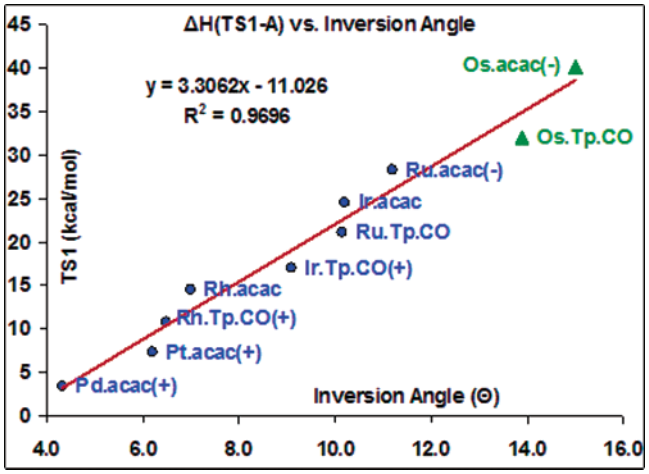

Figure 9. ΔH(TS1−A) versus inversion angle (Θ) in the olefin complex A.

estimate the insertion barrier from the geometric parameters in a structure from experiment or computation. This is currently under evaluation. We do expect metals with other electronic configurations than the d^6 evaluated here to exhibit similar relationships, although most likely with different coefficients. Indeed, Schmid and Ziegler suggest a relation between back-bonding and insertion barrier for metal complexes with d^1−d^4 configurations based on orbital analysis and olefin complexation energies.[23] However, Schmid and Ziegler do not demonstrate any linear relationships, most likely because olefin complexation energies depend on both forward and back-bonding.

With these observations in hand, we conclude that the relative ΔH values of TS1−A and TS2−D are linearly correlated with the accessibility of the M^{n+2} state of the system. The greater activity of the Tp·CO ligand set can thus be traced to a better balance between TS1 and TS2, most likely caused by the π-accepting qualities of the CO ligand. Removing electron density from the filled metal d-orbital stabilizes said orbital, and the M^{n+2} state becomes less accessible. A simple test of this explanation is replacement of the CO with a non-π-accepting ligand, such as NH_3. Calculations on the complex Ru·Tp·NH_3 reveal that ΔH(TS1−A) = 25.7 kcal/mol and ΔH(TS2−D) = 10.2 kcal/mol, as compared to 21.1 and 18.0 kcal/mol, respectively, for Ru·Tp·CO, and the explanation thus appears valid.

Further complicating this mechanism is a conclusion from our previous work.[6] To continue on the catalytic pathway, the system must open up a vacant site for benzene to coordinate (intermediate C in Figure 3). However, in the presence of olefin, there is a competition between olefin and benzene for coordination to the vacant site, as illustrated in Figure 10. Because the coordination is barrierless, we believe that the outcome of this competition is purely statistical; that is, at low concentrations of olefin mainly benzene will coordinate. For Ir·acac, we found that when olefin does coordinate, TS2 becomes the rate-determining step, ∼2 kcal/mol higher in energy than TS1. Furthermore, the coordinated olefin can undergo a second insertion, TS3, instead of C−H activation, although this pathway is kinetically inaccessible in the Ir·acac system. These conclusions correspond very well to the experimental observations that increased olefin concentration decreases the reaction rate at olefin:benzene ratios above 1:4 and that no oligomerization occurs.

In our previous report on the Ru·Tp·CO system,[8] we suggested from preliminary calculations that significant oligomerization would occur with this system, albeit most likely undetectable at the low olefin pressures used (0.17 MPa, corresponding to an olefin mole fraction of ∼0.01,[24] and thus approximately 1% of converted product should be butyl-benzene based on our statistical model[6]). We have since completed our theoretical studies on this system and find that a second insertion is favored over C−H activation by 6.7 kcal/mol for Ru·Tp·CO. These predictions have also been experimentally verified: at 1.7 Mpa of ethane, ∼15% butyl-benzene is observed,[9] while the statistical model[6] predicts ∼12%.

Because A → TS1 → B and G → TS3 → H are both olefin insertions, we expect that any system with a low-energy TS1 would also have a low-energy TS3 and thus be prone to oligomerization/polymerization. This is confirmed by the results summarized in Table 3, as ΔH(TS3−G) is uniformly ∼10 kcal/mol higher than the ΔH(TS1−A).

Moreover, because we have established that ΔH(TS2−D) increases as ΔH(TS1−A) decreases, a system with a low-energy TS1 would not lead to TS2 as a new rate-determining step, but would instead yield a system in which TS3 is lower in energy than TS2, as illustrated above with Ru·Tp·CO. Because a commercial hydroarylation catalyst must be able to operate under high olefin pressures, we elected to investigate whether this deduction is valid and whether a limit can be defined beyond which the system will be a polymerization catalyst.

The relevant quantity is the difference in energy between TS2 and TS3. If ΔH(TS2−TS3) < 0, the system should favor oligomerization, while ΔH(TS2−TS3) > 0 should favor hydroarylation. Plotting ΔH(TS1−A) versus ΔH(TS2−TS3) in Figure 11 shows how the relative energy of TS1 influences ΔH(TS2−TS3) and confirms that improving ΔH(TS1−A) does lead to negative ΔH(TS2−TS3) and thus oligomerization. It also shows that the relation between ΔH(TS1−A) and ΔH(TS2−TS3) is linear, obviating the design of systems for which ΔH(TS1−A) is improved while oligomerization is avoided.

A final concern for these systems was the possibility of β-hydride elimination from complex B, and the subsequent production of styrene. Experimentally, neither the Ir·acac system nor the Ru·Tp·CO system generates any measurable amounts of β-hydride elimination, and our analysis of the Ir·acac system showed that while β-hydride elimination is facile, loss of the produced styrene was significantly higher in energy than C−H activation (ΔH = 28.5 kcal/mol, $\Delta\Delta H$ = 8.0 kcal/mol) and the formed product simply reverts to complex B.

Calculations on the Ru·Tp·CO system show the same pattern: β-hydride elimination from complex B has an activation energy of merely 4.2 kcal/mol, but the dissociation of styrene has a barrier of 27.0 kcal/mol. However, the difference in the activation energies for the loss of styrene and C−H activation is merely 3.9 kcal/mol, once again a reflection of the above relationships. While the less accessible M^{n+2} state causes the C−H activation to be higher in energy, the loss of styrene is more facile due to less tightly coordinating olefins.

(23) Schmid, R.; Ziegler, T. *Organometallics* **2000**, *19*, 2756.

(24) Kozorezov, Yu. I.; Rusakov, A. P.; Pikalo, N. M. *Khim. Prom. (Moscow)* **1969**, *45*, 343.

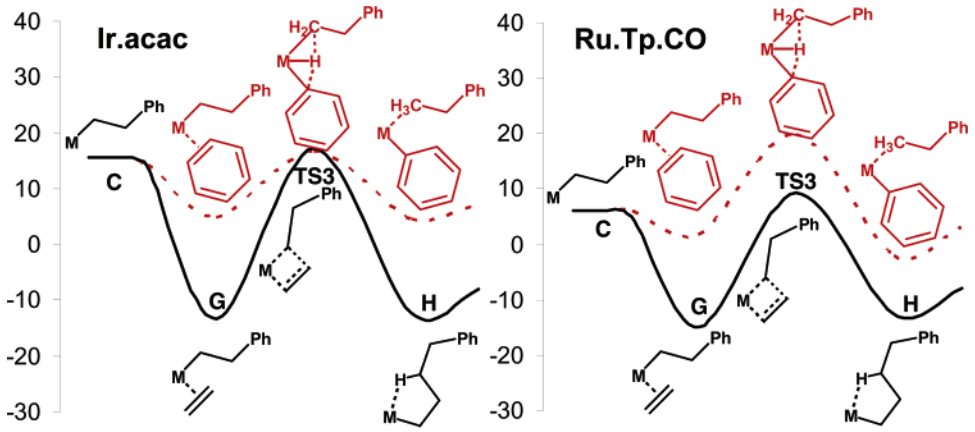

Figure 10. Competitive coordination and subsequent reaction of benzene (dotted line) and olefin (solid line).

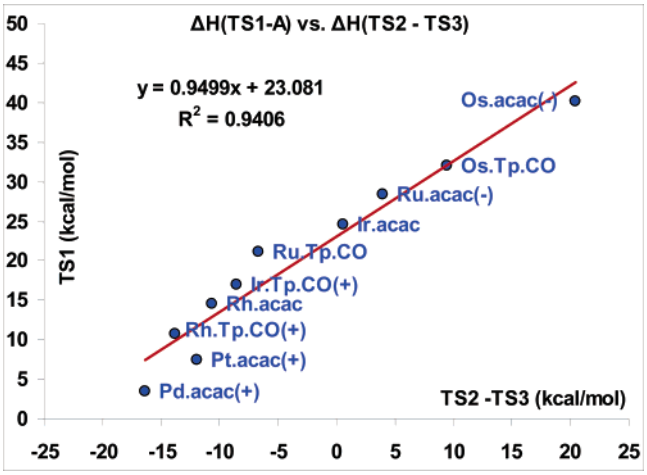

Figure 11. ΔH(TS1−A) versus ΔH(TS2−TS3).

These results do indicate that the systems with low insertion energy and high C−H activation energy, like Rh·Tp·CO$^+$ or Pt·acac$^+$, could potentially generate styrene. However, this would require the scavenging of the resulting hydride, and the energetics of this process is beyond the scope of the current study. Furthermore, these systems are already not suitable as hydroarylation catalysts due to the aforementioned propensity for oligomerization.

4. Conclusions

In light of these relationships, the obvious question must be asked: Are efficient insertion and C−H activation mutually exclusive? Based on the line in Figure 5, the "theoretical maximum" is a system where ΔH(TS1−A) = ΔH(TS2−D) = 18.6 kcal/mol. However, this system would still face problems with polymerization, and because TS3 appears to be roughly 10 kcal/mol higher in energy than TS1, a more practical limit appears to be ΔH(TS1−A) = ΔH(TS2−D) + 10 kcal/mol = 23.7 kcal/mol, ΔH(TS2−D) = 13.7 kcal/mol. Because this coincides almost exactly with the characteristics of Ir·acac, this does not leave much room for improvement, and the question becomes: Will all systems necessarily stay on the line?

Certainly, modifications of the π framework are likely to be futile, as they will directly influence the accessibility of the M^{n+2} state. Likewise, trying to tailor the metal to a particular ligand set (i.e., Ru for the Tp·CO, Ir for the acac) will likely yield the same result. However, one option remains to be explored: modification of the σ framework. Because the number of σ bonds in A → TS1 remains essentially unchanged while the number of σ bonds in D → TS2 increases by at least one full bond, it is plausible that changing the σ framework of the ligand set could influence TS1 and TS2 in varying amounts.

In our previous study of the Ir·acac system, we predicted that substituting the acac's with several electron-withdrawing CF_3 groups would lead to ΔH(TS1−A) = 21.6 kcal/mol, and we suggested that this system would be a more active catalyst.[6] Extending the investigation of Ir·acac−4CF_3 to include ΔH(TS2−D), we find that ΔH(TS2−D) = 14.0 kcal/mol, 2.2 kcal/mol higher than Ir·acac. While this does follow the trend outlined above, the increase in ΔH(TS2−D) is not as large as the increase for Ru·Tp·CO. This shows that manipulating the σ framework can move the system below the line in Figure YY5. Conceivably further changes in the σ framework might be even more effective and could lead to commercial catalyst.

Another possibility to obtain commercial catalysts would be to circumvent the relationship altogether. This could be done through any of the following:

(i) systems where C−H activation occurs via σ-bond metathesis or electrophilic addition;

(ii) di/multinuclear systems where insertion and C−H activation occurs at different nuclei; or

(iii) systems where the ligand set can change character in a fluxional pattern, catalyzing insertions in one conformer and C−H activation in another. However, to prevent polymerization, such a system must be designed such that the mode where C−H activation is enabled is the ground state and the mode where insertion is enabled is the high-energy conformer.

Finally, it should be noted that this is by necessity a simplified analysis of the hydroarylation mechanism. The barriers calculated here are lower bound barriers, because all ground-state and Curtin−Hammet effects are ignored. However, because these effects could only raise the relevant barriers, they would only have to be considered if a previous screening of ΔH(TS1−A) and ΔH(TS2−D) generated promising barriers.

5. Summary

This study shows a linear correlation between the activation energy for the 1,2-insertion and C−H activation steps in mononuclear late-metal complexes. This linear relationship occurs because both steps are directly influenced by the accessibility of the second higher oxidation state, M^n → M^{n+2}.

(i) Systems with an easily accessible M^{n+2} state activate C−H bonds easily through an oxidative addition or OHM process, while suffering from high-energy insertion transition states due to significant back-bonding of the olefin complex ground state.

(ii) Systems without an easily accessible M^{n+2} state (such as systems based on Pt^{IV}) have no debilitating back-bonding and consequently lead to a facile insertion step. However, these systems are not effective at activating the C−H bond, leading instead to polymerization.

We also show a linear correlation between the hybridization of the bound olefin and the activation energy for insertion. As hybridization is dependent on the amount of back-bonding to the olefin, these relationships translate into correlations between the amount of back-bonding and activation energy/thermodynamics.

Systems with a low-energy insertion step and a high-energy C−H activation step will exclusively yield polymerization. Furthermore, a system where the ΔH of the insertion step is between 1 and 2 times larger than the ΔH of the C−H activation step will suffer from oligomerization at higher olefin concentrations, caused by competitive olefin coordination in the catalytic cycle.

Preliminary work suggests that modifications of the σ framework can move the linear correlation described above. Substituting the $-CH_3$ groups on the Ir·acac system with $-CF_3$ groups reduces the energy of the insertion step to the same level as the Ru·Tp·CO system while increasing the energy of the C−H activation half as much as Ru·Tp·CO. Barring modifications of the σ framework, an efficient hydroarylation catalyst would most likely require a mechanistic paradigm shift.

Acknowledgment. We gratefully acknowledge financial support of this research by the ChevronTexaco Energy Research and Technology Co., and we thank Dr. Michael Driver and Dr. William Schinski of ChevronTexaco for helpful discussions. We also wish to thank Robert Nielsen, Guarav Bhalla, and Dr. Xiang Yang Liu for suggestions and insights.

Supporting Information Available: Tables of geometries, ZPE corrections, and absolute energies of intermediates A, B, D, E, and G, as well as geometries, ZPE corrections, absolute energies, and imaginary frequencies of transition states TS1, TS2, and TS3. This material is available free of charge via the Internet at http://pubs.acs.org.

JA048841J